

Structural characterization and magnetic properties for the semiconducting semimagnetic system $\text{Cu}_2\text{Cd}_{1-z}\text{Mn}_z\text{GeSe}_4$ alloys

E. Quintero^{a,*}, R. Tovar^a, M. Quintero^a, M. Morocoima^a, J. Ruiz^a, G. Delgado^b, J.M. Broto^c, H. Rakoto^c

^aCentro de Estudios de Semiconductores, Departamento de Física, Facultad de Ciencias, Universidad de los Andes, Mérida 5101, Venezuela

^bLaboratorio de Cristalografía, Departamento de Química, Facultad de Ciencias, Universidad de los Andes, Mérida 5101, Venezuela

^cLPMC-SNCMP INSA Complexe Scientifique de Rangueil, F-31077 Toulouse-Cedex, France

Abstract

X-ray powder diffraction measurements, at room temperature, and magnetic susceptibility χ measurements in the temperature range from 2 to 300 K, were made on polycrystalline samples of $\text{Cu}_2\text{Cd}_{1-z}\text{Mn}_z\text{GeSe}_4$ alloys. The X-ray diffraction patterns were used to show the equilibrium conditions and to determine lattice parameter values. Two single solid-phase fields were observed, viz. the stannite tetragonal structure (142 m) for alloys with $0 < z < 0.2$, and the wurzstannite structure (Pmn2₁) for samples $0.2 < z < 1.0$. The reciprocal of the susceptibility $1/\chi$ vs. T data showed that the samples have antiferromagnetic behavior. Values of the magnetic transition Néel temperature T_N were determined for the minimum in $1/\chi$ curves at lower temperatures. © 2002 Elsevier Science B.V. All rights reserved.

Keywords: Semimagnetic semiconducting alloys; Critical temperature

1. Introduction

Magnetic semiconducting compounds and alloys in which manganese is one of the component elements are of interest because of the large magneto-optical effects, which can occur in these materials. The materials which have been most studied are the semimagnetic semiconductor alloys obtained from the tetrahedrally coordinated $\text{A}^{\text{II}}\text{B}^{\text{VI}}$ semiconductor compounds by replacing a fraction of the group II cations with manganese, giving alloys which show spin-glass behavior, very

large magneto-optical effects, etc. [1]. It was suggested [2–4] that larger magneto-optical effects than those for the II–VI derived alloys could be obtained in materials in which the antiferromagnetic interaction between nearest-neighbor magnetic ions was smaller, and the interaction between ions on the same magnetic sublattice was greater. One set of materials which could satisfy these conditions were the tetrahedrally bonded $\text{A}_2^{\text{II}}\text{B}^{\text{II}}\text{C}^{\text{IV}}\text{D}_4^{\text{VI}}$ compounds by replacing the group II cations by Mn, Fe, Co and/or Ni ions [5–9]. It was shown that in almost all cases, the compound investigated showed an ordered structure based on either tetragonal, with the stannite structure, or orthorhombic structure [6–8].

*Corresponding author. Fax: +58-274-240-1286.

E-mail address: equinter@ciens.ula.ve (E. Quintero).

The aim of this paper is to show some results of the initial work on the crystallographic and magnetic properties of these materials. Here, results of X-ray powder diffraction, at room temperature, and magnetic susceptibility as a function of temperature on the $\text{Cu}_2\text{Cd}_{1-z}\text{Mn}_z\text{GeSe}_4$ alloys over the whole range of solid solution are presented.

2. Sample preparation and experimental techniques

The samples used in this work were prepared by the melt and anneal technique as described elsewhere [10]. Powder diffraction technique was employed in this study, using Ni-filtered $\text{Cu K}\alpha$ radiation. The diffracted intensities were recorded on a Bruker AXS diffractometer at room temperature in θ/θ reflection mode. The pattern was scanned over the angular range $15\text{--}100^\circ$ (2θ) with a step size of 0.02° and counting time of 25 s.

For each sample, magnetic susceptibility χ measurements as a function of temperature in the range 2–300 K were made using a Quantum Design MPMS-5 SQUID magnetometer with an external magnetic field of 100 G.

3. Results and discussion

The X-ray powder diffraction patterns showed sharp diffraction lines indicating that the samples were in good equilibrium conditions. The diffraction patterns, obtained for each sample, were indexed with the computer program DICVOL91 [11] using an absolute error of 0.03° (2θ) in the calculations. The results showed that two single solid-phase fields, viz. the stannite tetragonal structure ($I\bar{4}2m$) for the samples with $0 < z < 0.2$, while the rest of the samples $0.2 < z < 1.0$ have an orthorhombic superstructure of wurtzite which is known as wurzt-stannite ($\text{Pmn}2_1$). Appropriate lattice parameters values were determined for all samples, and the variation of the parameters with the manganese concentration is shown in Fig. 1. The result for the terminal compounds $\text{Cu}_2\text{Cd-GeSe}_4$ and $\text{Cu}_2\text{MnGeSe}_4$ are in good agreement

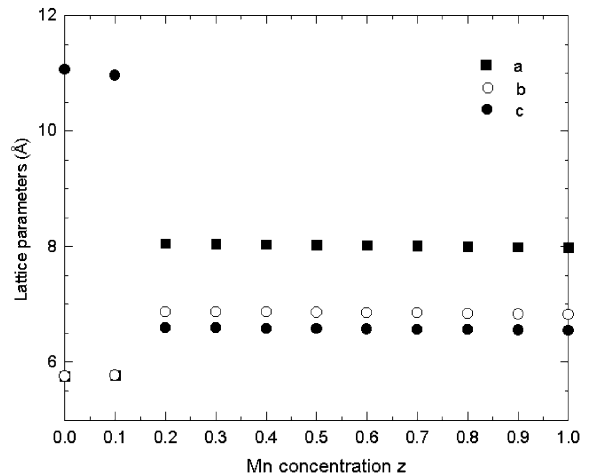


Fig. 1. Lattice parameters of $\text{Cu}_2\text{Cd}_{1-z}\text{Mn}_z\text{GeSe}_4$ as a function of concentration z .

with those reported previously [8,9]. It is seen that, within the limits of experimental error, the variation of the lattice parameters with z can be taken as linear for each single-phase field, and the slope discontinuities of the graphs give a good indication of the boundary between the single-phase fields.

Magnetic susceptibility: measurements of low-field magnetic susceptibility χ as a function of temperature were made on the samples shown by the X-ray measurements to be single phase. The resulting graphs of $1/\chi$ vs. T were found to be very similar to those reported previously for this type of alloy [12,13]. In all cases, the linear regions of the $1/\chi$ vs. T graphs were extrapolated to obtain values of the Curie–Weiss temperature θ . For samples with $z > 0.1$, the $1/\chi$ vs. T curves are of type ideal antiferromagnetic, giving a linear form down to the Néel temperature. This is illustrated in Fig. 2 for the sample of composition $z = 0.9$. The values of C , θ and T_N obtained from the experimental data for all the samples are given in Table 1.

Values of the magnetic transition Néel temperature T_N were determined for the minimum in $1/\chi$ at lower temperatures, as shown in Fig. 3, and these are seen to be in the same range of temperature as previously observed [14] for such materials. As has been seen for other similar alloys

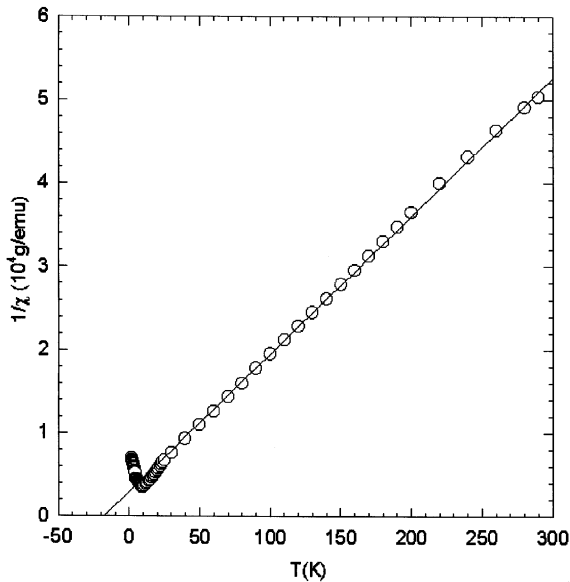


Fig. 2. Variation of $1/\chi$ with temperature for typical $\text{Cu}_2\text{Cd}_{1-z}\text{Mn}_z\text{GeSe}_4$ alloys with $z = 0.9$.

Table 1

Magnetic parameters for the $\text{Cu}_2\text{Cd}_{1-z}\text{Mn}_z\text{GeSe}_4$ alloys. Curie constant $C(\text{exp})$ and Curie–Weiss temperature θ , as obtained from fits to $\chi = C/(T - \theta)$

z	$C(\text{exp})$ (emu K/g)	$C(\text{theor})$ (emu K/g)	θ (K)	T_N (K)
1	7.53×10^{-3}	7.53×10^{-3}	-21.1	10.50
0.9	6.04×10^{-3}	6.72×10^{-3}	-17.9	9.20
0.8	4.89×10^{-3}	5.93×10^{-3}	-14.5	7.80
0.7	5.13×10^{-3}	5.15×10^{-3}	-9.9	7.00
0.6	4.00×10^{-3}	4.38×10^{-3}	-8.9	5.80
0.5	2.95×10^{-3}	3.62×10^{-3}	-6.5	4.40
0.4	2.59×10^{-3}	2.87×10^{-3}	-4.5	3.00
0.3	1.87×10^{-3}	2.14×10^{-3}	-2.8	—
0.2	1.25×10^{-3}	1.41×10^{-3}	-0.7	—
0.1	0.59×10^{-3}	0.7×10^{-3}	-0.3	—

$C(\text{theor})$ are theoretical values for the Curie constant assuming that the magnetic data is given by the spin only (S) contribution. Values of the magnetic transition Néel temperature T_N were determined for the minimum in $1/\chi$ curves at lower temperatures.

[15,16], extrapolation of the linear region of T_N vs. z to $T_N = 0$ gives a value for the nearest-neighbor percolation limit. Extrapolation of the line in Fig. 3, gave a value $z = 0.14$ for the orthorhombic phase.

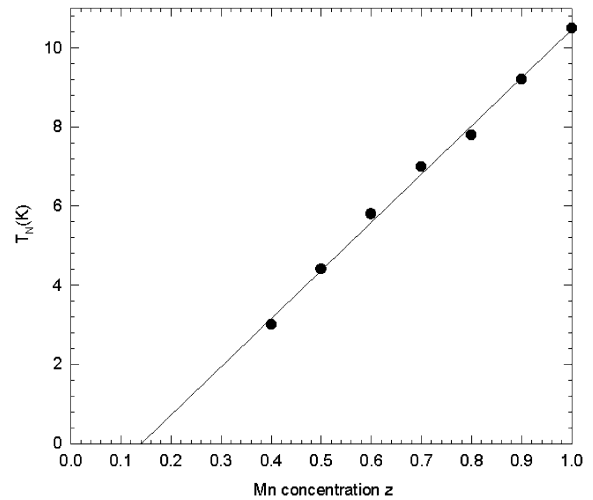


Fig. 3. Variation of the Néel temperature T_N with composition z for the $\text{Cu}_2\text{Cd}_{1-z}\text{Mn}_z\text{GeSe}_4$ alloys.

Acknowledgements

This work was supported by PCP (France)-CONICIT (Venezuela) Nanomaterials, CDCHT-ULA. Grants C-1013-00-A and C-951-99-05-B, Programa Postgrado Nacional Integrado en Física-CONICIT and CONICIT, Grant LAB-97000821.

References

- [1] J.K. Furdyna, J. Kossut, in: R.K. Willard son, A.C. Beer (Eds.), *Diluted Magnetic Semiconductors and Semimetal*, Vol. 25, Academic Press, New York, 1988 (Chapter 1).
- [2] P.A. Wolff, L.R. Ram-Mohan, *Mater. Res. Soc. Symp. Proc.* 89 (1987) 1.
- [3] P.A. Wolff, D. Heimann, E.D. Isaac, P. Becla, S. Foner, I.R. Ram-Mohan, D.H. Ridgley, K. Dwight, D. Wold, in: G. Landwehr (Ed.), *High Magnetic Fields in Semiconductors Physics*, Springer, Berlin, 1988.
- [4] Y. Shapira, E.J. McNiff Jr., N.F. Oliveira Jr., E.D. Honing, K. Dwight, A. Wold, *Phys. Rev. B* 37 (1988) 411.
- [5] R. Nitsche, D.F. Sargent, P. Wild, *J. Cryst. Growth* 1 (1967) 52.
- [6] E. Parthe, K. Yvon, R.H. Deich, *Acta Cryst. B* 25 (1969) 1164.
- [7] J. Allemand, M. Wintenber, *Bull. Soc. FR Mineral. Crystallogr.* 93 (4) (1970) 14.
- [8] W. Schafer, R. Nitsche, *Mater. Res. Bull.* 9 (1974) 645.
- [9] L. Guen, W.S. Glaunsinger, *J. Solid State Chem.* 35 (1980) 10.

- [10] R. Tovar, M. Quintero, P. Grima, J.C. Woolley, *Phys. Stat. Sol. (a)* 111 (1989) 405.
- [11] A. Boulif, D. Louer, *J. Appl. Cryst.* 24 (1991) 987.
- [12] J.C. Woolley, S. Bass, A.-M. Lamarche, G. Lamarche, M. Quintero, M. Morocoima, P. Bocaranda, *J. Magn. Mater.* 150 (1995) 353.
- [13] M. Quintero, M. Morocoima, A. Rivero, P. Bocaranda, J.C. Woolley, *J. Phys. Chem. Solids* 58 (1997) 491.
- [14] X.L. Chen, A.-M. Lamarche, G. Lamarche, J.C. Woolley, *J. Magn. Mater.* 118 (1993) 119.
- [15] J.C. Woolley, S. Bass, A.-M. Lamarche, M. Quintero, M. Morocoima, P. Bocaranda, *J. Magn. Mater.* 150 (1995) 353.
- [16] M. Quintero, P. Grima, J.E. Avon, B. Lamarche, J.C. Woolley, *Phase Diagram, Phys. Stat. Sol. (a)* 108 (1988) 599.